Excited Singlet (S_1) State Interactions of 6,11-Dihydroxy-5,12-naphthacenequinone with Aromatic Hydrocarbons

M. C. Rath, H. Pal,* and T. Mukherjee

Radiation Chemistry & Chemical Dynamics Division, Bhabha Atomic Research Centre, Trombay, Mumbai 400 085, India

Received: September 21, 2000; In Final Form: May 1, 2001

Interaction in the excited singlet state (S_1) of 6,11-dihydroxy-5,12-naphthacenequinone (DHNQ) with aromatic hydrocarbons (AH) has been investigated using steady-state (SS) and time-resolved (TR) fluorescence quenching measurements. In both nonpolar (cyclohexane; CH) and polar (acetonitrile; ACN) solvents, the fluorescence quenching of DHNQ by AHs is accompanied with the appearance of exciplex emissions. The emission maxima of the exciplexes correlate linearly with both ionization potentials (IP) and oxidation potentials {$E(AH/AH^{\cdot+})$} of the quenchers (AH), indicating the charge transfer (CT) type of interaction between the S_1 state of DHNQ (acceptor) and the ground state of the AHs (donor). The kinetic details of the exciplex formation have been evaluated by analyzing the SS and TR fluorescence quenching results at different temperatures following a suitable mechanistic scheme. Picosecond laser flash photolysis (LFP) studies on the DHNQ−AH systems show a major transient absorption band in the 530 to 630 nm region along with a weak long-wavelength absorption tail. The transient lifetimes for the 530−630 nm absorption band are very similar to the exciplex lifetimes estimated from the fluorescence quenching results. At the long wavelength absorption tail, the transient lifetime could not be estimated due to very weak absorption. It is inferred that the 530−630 nm transient absorption band is mostly due to the $S_1 \rightarrow S_n$ transition. The long wavelength absorption tail has been attributed to the anion radical of DHNQ, drawing an analogy with the anion radical absorption spectrum of 1,4-dihydroxy-9,10-anthraquinone (quinizarin; QZ), a lower analogue of DHNQ. The picosecond LFP results largely correlate with the results obtained from the fluorescence quenching studies.

1. Introduction

Hydroxy and amino substituted quinones have immense importance in the dye industry,[1] biology,[2] and pharmaceutical chemistry.[3,4] Hydroxy quinones constitute the basic chromophoric part of a number of quinone-based antitumor agents, such as daunorubicin, adriamycin, etc. Radiation and photochemistry of these quinones have direct implications in understanding the activities of these antitumor agents in the biological systems.[5−7] A large number of hydroxy and amino substituted quinones have also been used as coloring materials for synthetic polymers such as nylons, polyesters, cellulose acetates, etc.[8,9] The hydroxy substituted quinones are in particular of considerable commercial importance in this respect due to their excellent light fastness properties on synthetic fibers.[9] Hydroxy and amino substituted quinones are also used as model probes for studying the effect of intra- and intermolecular hydrogen bonding on the photophysical properties of the excited states.[10−14] The presence of the hydroxy and amino substituents often causes the quinonoid compounds to have reasonably good fluorescence quantum yields (Φ_f), allowing their excited-state properties to be studied using fluorescence detection as a convenient tool.[10−14] Due to the presence of the quinone moiety, these compounds are also good electron acceptors, and have widely been studied by pulse radiolytic techniques for understanding their redox characteristics.[15−18]

Quinones and their derivatives are often used as the electron acceptors in studying the electron transfer (ET) processes under both intra- and intermolecular conditions.[19−24] The dynamics of ET reactions between the excited triplet states of differently substituted 1,4-benzoquinones and the ground states of aromatic hydrocarbons (AH) in acetonitrile (ACN) solutions have been reported recently by Hubig and Kochi.[22] Charge transfer (CT) and ET interactions in the excited S_1 states of a number of amino and hydroxy substituted 9,10-anthraquinones with both AHs and the amine donors have been investigated by us.[23,24] The 1,4-dihydroxy-9,10-anthraquinone (quinizarin; QZ) is the most studied compound among the hydroxyquinones used as a probe to investigate the photophysical properties and many other physicochemical processes.[10−14,23−25] Recently we have investigated the photophysical properties of 6,11-dihydroxy-5,12-naphthacenequinone (DHNQ), a higher analogue of QZ, in different solvents.[26] It has been observed that the Φ_f values of DHNQ in aromatic solvents are substantially lower than those in other nonaromatic solvents.[26] We explained these results by considering the exciplex formation between the S_1 state of DHNQ and the aromatic solvent molecules. In the present work, a systematic study has been carried out using both steady-state (SS) and time-resolved (TR) fluorescence quenching techniques to understand the exact nature of interaction between DHNQ and the AHs. Temperature effect on the fluorescence quenching dynamics has also been investigated to get more insight into the mechanism involved in these systems. Picosecond laser flash photolysis (LFP) experiments have also been carried out to understand the nature of the transients produced in the present systems following photoexcitation and thus to substantiate the

* Author to whom correspondence should be addressed. Fax: (+)91-22-5505151. E-mail: hpal@apsara.barc.ernet.in.

10.1021/jp003420j CCC: $20.00 © 2001 American Chemical Society
Published on Web 07/31/2001

inferences drawn from the fluorescence quenching studies. The chemical structure of DHNQ is shown below.

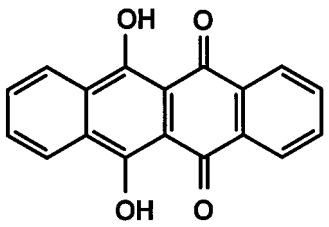

(DHNQ)

2. Materials and Methods

Purest grade DHNQ was obtained from Aldrich. The sample was further purified by repeated crystallization from methanol. All the AHs were of purest grade from either Aldrich, Fluka, Spectrochem India, or BDH. They were used without further purification. All the solvents were of spectroscopic grade from Fluka, BDH or Spectrochem India and used as received.

A Shimadzu model UV-160A spectrophotometer was used for the ground-state absorption measurements. A Hitachi model F-4010 spectrofluorimeter was used for all the SS fluorescence studies. The S_1 state energies of DHNQ (E_{00}^{Q}) in cyclohexane (CH) and acetonitrile (ACN) solutions were estimated from the intersection wavelengths of the normalized excitation and fluorescence spectra of the compound in the respective solvents. The S_1 state energies (E_{00}^{AH}) of the AHs were taken from the literature.[27] The E_{00}^{Q} and E_{00}^{AH} values of DHNQ and AHs are listed in Table 1.

Fluorescence lifetime measurements were carried out in a TR fluorescence spectrometer model 199 from Edinburgh Instruments, U.K. The instrument works on the principle of time-correlated single-photon-counting (TCSPC).[28] A hydrogen-filled thyratron-triggered coaxial flash lamp of having about 1.2 ns pulse width (fwhm) and 30 kHz repetition rate was used as the excitation source. The fluorescence decays were analyzed by reconvolution procedure,[28] using a proper instrument response function obtained by substituting the sample cell with a light scatterer. The observed decay curves were fitted as a mono-exponential function,

$$I(t) = B \exp(-t/\tau) \qquad (1)$$

where B is the preexponential factor and τ is the fluorescence lifetime. For all the monoexponential analysis, the chi-square (χ^2) values were found to be close to unity and the weighted residuals were randomly distributed among the data channels.[28] Biexponential analysis of the observed decays did not give any significant improvement in the χ^2 values as well as in the distribution of the weighted residuals, indicating the effective monoexponential behavior of the fluorescence decays.[28]

Picosecond laser flash photolysis experiments were carried out using a pump−probe transient spectrometer. The details of this instrument have been described elsewhere.[29] Briefly, the second harmonic output (532 nm, 8 mJ, 35 ps) of an active-passively mode-locked Nd:YAG laser (Continuum, USA, model 501-C-10) was used to excite the sample. A white light continuum (~450 to 900 nm), produced by focusing the residual fundamental (1064 nm) of the Nd:YAG laser onto a 10 cm path-length quartz cell containing 50:50 (v/v) H_2O-D_2O mixture, was used as the monitoring light source. The time-delay between the pump and the probe pulses was varied by using a 1 m long delay rail at the probe end. The probe pulse was bifurcated by using a 50:50 beam splitter to generate the reference and the analyzing beams. Both the reference and the analyzing beams were dispersed through a spectrograph and recorded by a dual diode array based optical multichannel analyzer interfaced to an IBM-PC.

TABLE 1: The Photophysical and Electrochemical Properties of the Acceptor (DHNQ) and the Donors (AHs) Used in This Study

acceptor	E_{00}^{Q} in CH (eV)[a]	E_{00}^{Q} in ACN (eV)[a]	$E(Q/Q^{-})$ vs Ag/Ag^{+} (V)
DHNQ	2.38	2.37	−1.4
donors	E_{00}^{AH} (eV)[b]	IP (eV)[c]	$E(AH/AH^{\cdot+})$ vs Ag/Ag^{+} (V)[d]
BZ	4.77	9.24	2.00
TOL	4.62	8.82	1.68
XYL	4.52	8.44	1.56
MES	4.55	8.40	1.55
TMB	4.35	8.03	1.29
PMB	4.35	7.92	1.28
HMB	4.33	7.85	1.16

[a] Estimated from the intersecting wavelengths of the normalized fluorescence and excitation spectra. [b] Taken from ref 27. [c] Taken from ref 30. [d] Taken from ref 31.

A potentiostat−galvanostat, model PGSTAT 20, from ECO CHEMIE, Netherlands, was used for the cyclic voltammetric measurements. The reduction potential $\{E(Q/Q^{\cdot-})\}$ of DHNQ was determined in ACN solution using 0.1 mol dm^{-3} tetraethylammonium perchlorate as the supporting electrolyte, glassy carbon as the working electrode, and $Ag/AgCl/Cl^{-}$ (3.0 mol dm^{-3} of Cl^{-}; standard reduction potential is +0.22 V,[30]) as the reference electrode. The value thus measured was normalized with respect to the Ag/Ag^{+} electrode (standard reduction potential is +0.79 V,[30]). The oxidation potentials of the AHs, $E(AH/AH^{\cdot+})$, against Ag/Ag^{+} electrode in ACN were taken from the literature.[31] The $E(Q/Q^{\cdot-})$ and $E(AH/AH^{\cdot+})$ values in ACN for DHNQ and the AHs are listed in Table 1. Table 1 also lists the ionization potentials (IP) of the AHs as obtained from the literature.[30]

3. Results and Discussion

3.1. Steady-State Fluorescence Quenching. The fluorescence intensity and the shape of the fluorescence spectra of DHNQ in both CH and ACN undergo substantial changes in the presence of the AHs, namely, benzene (BZ), toluene (TOL), *p*-xylene (XYL), mesitylene (MES), 1,2,4,5-tetramethylbenzene (TMB), pentamethylbenzene (PMB), and hexamethylbenzene (HMB). As the concentration of the AHs is increased in the solution, the intensity of the observed fluorescence gradually decreases. However, there is a concomitant change in the shape of the emission spectra with the AH concentration, indicating a relative increase in the fluorescence intensity at the longer wavelength region of the observed emission spectra. It is evident from the spectral changes that in the presence of AHs a newly formed species contributes with an overlapping emission along with the fluorescence of DHNQ, especially at the longer wavelength region of the observed emission spectra. Typical SS fluorescence results for the DHNQ−MES pair in ACN are shown in Figure 1, indicating both the DHNQ fluorescence quenching and the concomitant changes in the spectral shape in the presence of the AH quencher.

For all the DHNQ−AH systems, the emission spectra of the newly formed species were obtained by subtracting the normalized fluorescence spectra of DHNQ in the absence of the AHs

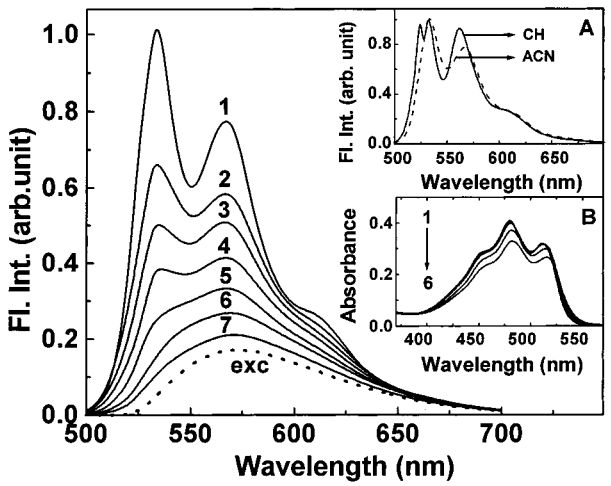

Figure 1. Observed fluorescence spectra of DHNQ in the presence of different concentrations of MES in acetonitrile (ACN). The MES concentrations are (**1**) 0, (**2**) 0.068, (**3**) 0.13, (**4**) 0.24, (**5**) 0.41, (**6**) 0.86, and (**7**) 1.44 mol dm^{-3}. Spectrum indicated by "exc" is the exciplex emission spectrum obtained for DHNQ−MES systems by subtracting the normalized fluorescence spectrum 1 from spectrum 7. The normalization was done at 520 nm. **Inset**: **(A)** Normalized fluorescence spectra of DHNQ in cyclohexane (CH) and ACN, indicating no significant shift in the spectra with solvent polarities. **Inset**: **(B)** Absorption spectra of DHNQ in the presence of different concentration of MES in ACN. The MES concentrations are: (**1**) 0, (**2**) 0.13, (**3**) 0.24, (**4**) 0.41, (**5**) 0.86, and (**6**) 1.44 mol dm^{-3}.

from the observed emission spectra in the presence of reasonably high concentration of the AHs. The normalization was always done at the blue edge of the DHNQ emission spectra (∼520 nm), where the exciplex emission is expected to be negligible compared to the DHNQ fluorescence. The emission spectra for the newly formed emissive species thus obtained were broad and structureless. We attribute these new broad emissions to the exciplexes formed between the excited state (S_1) of DHNQ and the ground state of AHs. Typical exciplex spectrum for DHNQ−MES pair is shown in Figure 1 with the curve designated as "exc".

At this point it is important to consider if the observed changes in the spectral shape in the DHNQ fluorescence spectra in the presence of the AHs are due to the associated small changes in the solvent polarities due to the presence of reasonably high concentrations of the AHs. That the marginal changes in the solvent polarities due to the presence of the AHs is not the cause for the observed changes in the fluorescence spectra is indicated from the fact that the fluorescence spectra of the parent molecule DHNQ do not change much with the solvent polarities. We plot in the Inset A of Figure 1 the fluorescence spectra of DHNQ in CH and ACN in absence of any AH for a comparison. It is evident from this figure that there is hardly any shift in the DHNQ fluorescence spectra from going from nonpolar solvent CH to polar solvent ACN except that in CH the spectrum is little more structured than in ACN. It is thus evident that the observed changes in the fluorescence spectra of DHNQ in the presence of the AHs must be due to the formation of emissive exciplex in these systems. Due to strong overlapping of the DHNQ and the exciplex emissions, it is not possible to estimate the exact fluorescence quantum yield for exciplexes (Φ_{exc}) except having just a semiquantitative estimate. Considering the fluorescence quantum yields (Φ_f) for DHNQ in CH and ACN as 0.53 and 0.42, respectively,[26] a semiquantitative estimate for Φ_{exc} values are made to be ∼ 0.14 and ∼0.09 for the DHNQ−MES pair in CH and ACN, respectively. For DHNQ−XYL and DHNQ−TMB pairs also the Φ_{exc} values seem to be almost in the similar range. For rest of the DHNQ−AH pairs the Φ_{exc} values seem to be much lower, probably due to much weaker exciplexes formed with BZ and TOL as the quenchers and faster nonradiative deactivation for the relatively stronger exciplexes formed with quenchers such as PMB and HMB.

As Table 1 indicates, the S_1 state energies of AHs ($E_{00}{}^{AH}$) are higher than that of DHNQ ($E_{00}{}^{Q}$). The energy transfer from the S_1 state of DHNQ to that of AHs is, therefore, highly endoergic. It is thus inferred that the singlet−singlet energy transfer cannot cause the fluorescence quenching of DHNQ by AHs. It is inferred from the observed spectral changes that the fluorescence quenching of DHNQ by AHs occurs via the formation of exciplexes as the intermediates in both nonpolar (CH) and polar (ACN) solvents.

It is seen for the present systems that the exciplex emission maxima ($\bar{\nu}_{exc}{}^{max}$) gradually shift toward longer wavelengths as the IP or the $E(AH/AH^{\cdot+})$ values of the AHs are reduced. In fact, the plots of $\bar{\nu}_{exc}{}^{max}$ vs IP or $E(AH/AH^{\cdot+})$ of the quenchers were linear for the present systems in both CH and ACN solutions. Typical $\bar{\nu}_{exc}{}^{max}$ vs $E(AH/AH^{\cdot+})$ plots in CH and ACN solutions for the DHNQ−AH systems are shown in Figures 2A and 2B, respectively. It is inferred from these results that the exciplexes in the present systems are formed by the charge transfer (CT) type of interaction between AHs and the S_1 state of DHNQ.

The effect of solvent polarity on the exciplex emission maxima for the present systems has also been investigated using different solvents and solvent mixtures. The exciplex emission spectra in these solvents were extracted using the subtraction method discussed earlier (cf. caption of Figure 1). It is seen that the $\bar{\nu}_{exc}{}^{max}$ values in different solvents shift toward longer wavelengths as the solvent polarity is increased. The $\bar{\nu}_{exc}{}^{max}$ values were correlated with the solvent polarity function (Δf) following the relation suggested by Beens et al. for exciplex emissions (eqs 2 and 3).[32]

$$\bar{\nu}_{exc}{}^{max} = \bar{\nu}_0{}^{max} - \frac{2\mu_{exc}{}^2}{hca^3}\Delta f \tag{2}$$

$$\Delta f = \left\{\frac{\epsilon - 1}{2\epsilon + 1}\right\} - \frac{1}{2}\left\{\frac{n^2 - 1}{2n^2 + 1}\right\} \tag{3}$$

where $\bar{\nu}_0{}^{max}$ is the hypothetical gas-phase exciplex emission frequency, μ_{exc} is the dipole moment of the exciplex, a is the interaction distance between the fluorophore and the quencher, ϵ is the static dielectric constant, and n is the refractive index of the solvent. The ϵ and n values for the pure solvents were taken from the literature.[30] For mixed solvents (MS), the ϵ and n values were calculated as[33−36]

$$\epsilon_{MS} = f_A\epsilon_A + f_B\epsilon_B \tag{4}$$

$$n_{MS}{}^2 = f_A n_A{}^2 + f_B n_B{}^2 \tag{5}$$

where the suffixes A and B represent the pure solvents A and B, respectively, and f_A and f_B are the volume fractions of the respective solvents. To be noted that the solvent polarity parameters estimated using ϵ_{MS} and n_{MS} values calculated using eqs 4 and 5 correlate nicely the different physicochemical parameters of a large number of systems.[29,33−39] It is seen for the present systems that the $\bar{\nu}_{exc}{}^{max}$ vs Δf plots are linear for all DHNQ−AH pairs within experimental error. A typical $\bar{\nu}_{exc}{}^{max}$

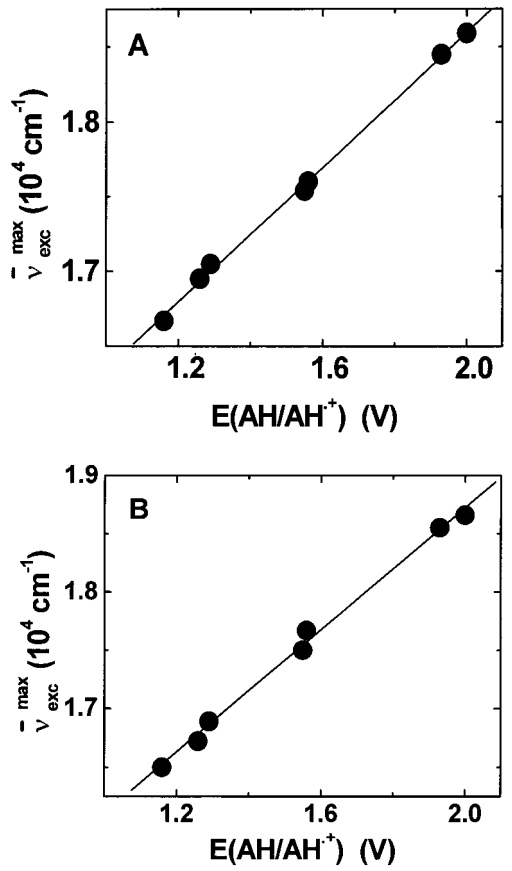

Figure 2. The $\bar{\nu}_{exc}^{max}$ vs $E(AH/AH^{\cdot+})$ plots for different DHNQ−AH pairs in (**A**) cyclohexane, and (**B**) acetonitrile. The linear correlation indicates the involvement of the CT interaction in the quenching mechanism.

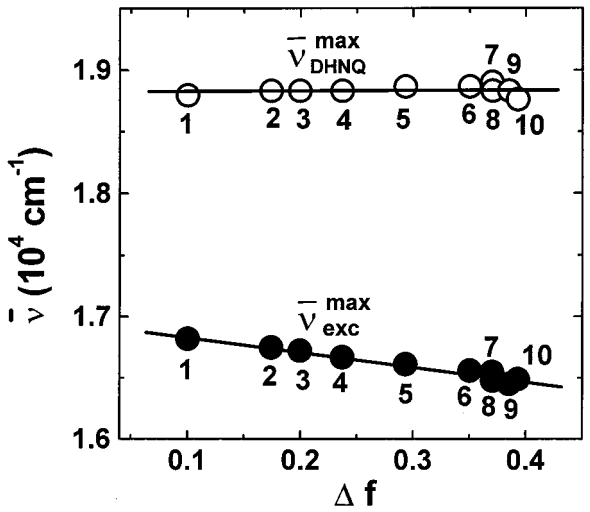

Figure 3. The $\bar{\nu}_{exc}^{max}$ vs Δf plot (cf. eqs 2 and 3) for DHNQ−HMB pair. The solvents are (**1**) cyclohexane (CH), (**2**) 8:2 (v/v) CH:ethyl acetate (EA), (**3**) 7:3 (v/v) CH:EA, (**4**) 5:5 (v/v) CH:EA, (**5**) EA, (**6**) 8:2 (v/v) EA:acetonitrile (ACN), (**7**) 2-propanol, (**8**) 6:4 (v/v) EA:ACN, (**9**) 3:7 (v/v) EA:ACN, and (**10**) ACN. The emission maxima of DHNQ ($\bar{\nu}_{DHNQ}^{max}$) have also been plotted vs Δf for the same solvents indicating no significant shift in $\bar{\nu}_{DHNQ}^{max}$ with solvent polarities.

vs Δf plot for a DHNQ−PMB pair is shown in Figure 3. The μ_{exc} values were obtained from the slopes of such plots, assuming the interaction distance a to be equal to the sum of the van der Waals' radii of the AHs and DHNQ, as estimated following Edward's volume addition method.[40] The value of μ_{exc} thus estimated for different DHNQ−AH pairs are listed in

TABLE 2: Dipole Moments of the Exciplexes (μ_{exc}) and the Temperature Coefficients of the Bimolecular Quenching Constants (ΔE_q) for Different DHNQ−AH Systems

		ΔE_q (kcal mol^{-1})	
AH	μ_{exc} (D)	CH	ACN
TOL		−5.1	−5.2
XYL	4.7	−5.3	−5.5
MES	5.0	−5.1	−5.3
TMB	5.3	−2.5	−2.9
PMB	6.1	−0.3	−0.1
HMB	6.6	1.7	1.2

Table 2. It is seen from this table that the μ_{exc} values in the present systems are not that high, only in the range of 4 to 7 D. The shifts in the exciplex emission maxima with the solvent polarity, however, indicate that the interaction between the S_1 state of DHNQ and the ground state of AHs is of CT in nature. This is also supported by the linear $\bar{\nu}_{exc}^{max}$ vs $E(AH/AH^{\cdot+})$ plots shown in Figure 2. It is important at this point to see if the emission maxima of DHNQ ($\bar{\nu}_{DHNQ}^{max}$) also shift toward longer wavelengths with solvent polarities and thus complicate the correlations of the $\bar{\nu}_{exc}^{max}$ values with Δf. It has been observed that the $\bar{\nu}_{DHNQ}^{max}$ does not shift to any great extent for the Δf range used for the estimation of the μ_{exc} values for the exciplexes. For a comparison the $\bar{\nu}_{DHNQ}^{max}$ vs Δf plot for DHNQ fluorescence for the same set of solvents as used for the exciplexes are shown in Figure 3. In DHNQ as well as in its lower analogue 1,4-dihydroxy-9,10-anthraquinone (quinizarin; QZ), there are strong intramolecular hydrogen bondings between the quinonoid and the hydroxyl groups, making quasiaromatic ring structures among the substituents.[7,10,25,26,41] Due to these quasiaromatic ring structures, the absorption and fluorescence spectra of these molecules do not show any significant shift with solvent polarities, except that the vibrational structures in the absorption and fluorescence spectra become blurred in polar solvents.[7,10,25,26,41]

The extent of CT between a donor and an acceptor during the exciplex formation is largely determined by the electron donating power of the former and the electron accepting power of the latter. It is usually seen that, when the donors and the acceptors are very strong so that the expected free energy changes ($\Delta G°$) for a complete ET are as negative as about 15 kJ mol^{-1} or more, the exciplexes are usually formed with a large extent of CT, giving μ_{exc} values in the range of about 14−15 D.[42] For weak donor−acceptor pairs, for which $\Delta G° \gg -15$ kJ mol^{-1}, the extent of CT and consequently the values of μ_{exc} are usually very low.[42] The dipole moment values of about 4 to 7 D (Table 2), as estimated for the exciplexes in the present systems, clearly indicate that the CT interaction between DHNQ and AHs is not that strong.

The solvent polarity is seen to have only a nominal effect on the observed exciplex emission intensities for all the DHNQ−AH systems. Though we could not estimate the exact exciplex emission yields in different solvents due to strong overlapping of the DHNQ and the exciplex emission spectra, it is seen qualitatively that for all DHNQ−AH pairs the exciplex emission intensity only marginally reduces on increasing the solvent polarity. Thus, for the present systems, reasonably good exciplex emissions are observed even in a strongly polar solvent like ACN in comparison to those observed in a strongly nonpolar solvent like CH. For the majority of the systems which show exciplex emissions in nonpolar solvents, it is usually seen that the exciplex emission vanishes in a strongly polar solvent such as ACN.[42−44] The present systems thus fall under those rare classes of the donor−acceptor pairs for which reasonable

TABLE 3: Bimolecular Quenching Rate Contstants (k_q) Determined for Different DHNQ−AH Systems in Cyclohexane (CH) and Acetonitrile (ACN) at Different Temperatures Using Steady-State Fluorescence Measurements

	CH[a] k_q (10^9 dm^3 mol^{-1} s^{-1})				ACN[a] k_q (10^9 dm^3 mol^{-1} s^{-1})			
AH	30 °C	40 °C	50 °C	60 °C	30 °C	40 °C	50 °C	60 °C
BZ	0.08	*b*	*b*	*b*	0.03	*b*	*b*	*b*
TOL	0.27	0.25	0.23	0.20	0.14	0.10	0.09	0.08
XYL	0.71	0.54	0.40	0.31	0.34	0.27	0.20	0.16
MES	1.81	1.41	1.11	0.86	1.23	0.95	0.72	0.54
TMB	5.69	5.38	5.02	4.68	8.62	7.51	6.62	5.53
PMB	9.80	9.70	9.50	9.32	11.52	11.47	11.45	11.42
HMB	10.30	11.40	12.10	13.50	15.10	16.12	17.20	18.11

[a] The fluorescence lifetimes (τ_0) of DHNQ in the absence of any quenchers are 5.23, 5.21, 5.19, and 5.18 ns in CH and 5.36, 5.35, 5.33, and 5.32 ns in ACN at temperatures of 30, 40, 50, and 60 °C, respectively. [b] The temperature effect on k_q values with BZ as the quencher could not be estimated accurately due to a very low fluorescence quenching rate.

exciplex emissions are also observed in a strongly polar solvent such as ACN.[42−44]

For most of the donor−acceptor systems, the exciplex formation in a strongly polar solvent such as ACN is usually very unlikely because in such a polar solvent, the direct ET from the donor to the acceptor often dominates over the exciplex formation process.[43−45] Further, in a polar solvent such as ACN, even if the exciplexes are formed, they are often very unstable and undergo quick ion-dissociation (ID) to form the solvent-separated ion-pairs (SSIP), making the exciplex emission often undetectable.[46] Observing exciplex emissions in the present systems in polar ACN solvent is thus quite an unusual phenomenon and in the literature such results in ACN solvent have been reported only for a limited number of systems.[42−44] It is indicated from the present results that for the DHNQ−AH systems, the direct ET from the donor to the acceptor or the ID of the exciplexes to form SSIP cannot suppress the exciplex emission to any appreciable extent as are observed for most of the donor−acceptor systems in polar ACN solvent. We will discuss on the extent of competition between direct ET and the exciplex formation mechanism in the present systems later in section 3.5.

It is seen that for the lower concentration range of the quenchers (∼0.1 to ∼0.5 mol dm^{-3}; depending on the strength of interaction of the AHs), there is hardly any change in the longer wavelength absorption band of DHNQ. With high concentrations of the AHs (>1 mol dm^{-3}), however, the longer wavelength edge of DHNQ absorption spectra becomes little extended along with a slight reduction in the absorbance at the absorption peak. These results thus indicate the formation of some weak ground-state complexes between DHNQ and AHs. The absorbance changes in the absorption spectra of DHNQ in the presence of AHs are, however, not that large to analyze with confidence to extract out the parameters related to the ground-state complex formation. Typical results on the ground-state absorption spectra for DHNQ−MES system in ACN are shown in Inset B of Figure 1.

Keeping in mind the possible effects of the ground-state complex formation and the overlapping exciplex emissions with the DHNQ fluorescence, a number of precautions were taken in estimating the parameters related to quenching kinetics using the SS fluorescence measurements. The excitation wavelength was chosen at the shorter wavelength edge of DHNQ absorption spectrum (i.e., at 480 nm), where the ground-state complexes

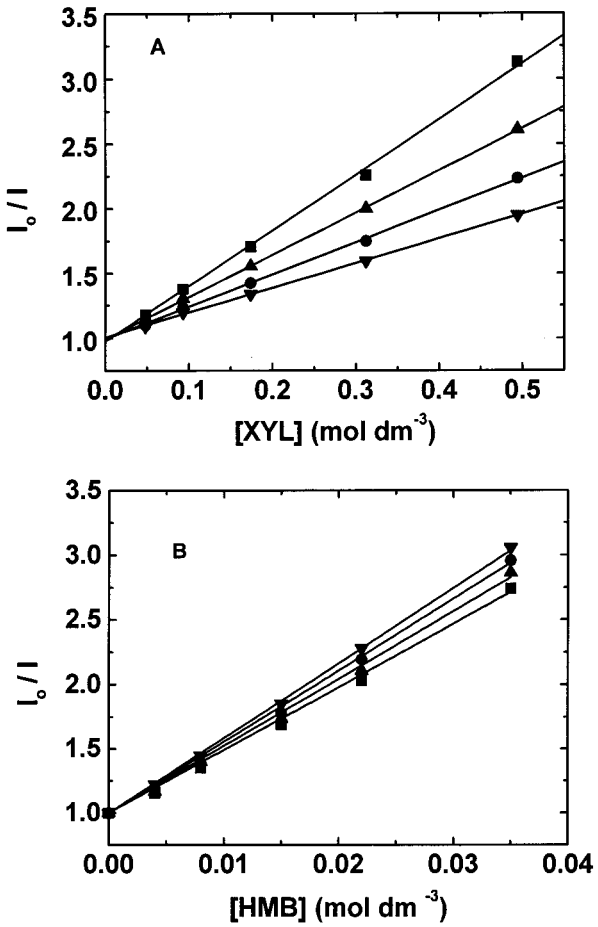

Figure 4. Typical Stern−Volmer plots (I_0/I vs [Q]; cf. eq 6) obtained from steady-state fluorescence quenching studies in (**A**) DHNQ−XYL and (**B**) DHNQ−HMB systems in cyclohexane at different temperatures; 30 °C (■), 40 °C (▲), 50 °C (●), and 60 °C (▼).

are expected to have very little absorption (cf. Inset B of Figure 1). The quencher concentrations were also kept low enough (∼0.1 to ∼0.5 mol dm^{-3}; depending on the strength of interaction of the AHs) for all the measurements so that the extent of the ground-state complex formation is as such small. With low quencher concentrations used, the effect of the exciplex emissions is also not that high on the observed fluorescence spectra. Further, the quenching of the fluorescence intensity was always monitored at the 0−0 vibrational band of DHNQ fluorescence spectra (i.e., at ∼532 nm). It is expected that the contribution from the exciplex emissions at the 0−0 vibrational band of DHNQ fluorescence spectra will be quite less and thus not introduce much error in the estimation of the parameters related to the quenching kinetics in the present systems.

Within the low concentration limit of the quenchers (∼0.1 to ∼0.5 mol dm^{-3}, depending on the strength of interaction of the AHs), the SS fluorescence quenching of DHNQ, as measured at the 0−0 vibrational band of the fluorophore, followed the linear Stern−Volmer (SV) relationship (eq 6):[47]

$$\frac{I_0}{I} = 1 + K_{SV}[Q] = 1 + k_q\tau_0[Q] \qquad (6)$$

where I_0 and I are the relative fluorescence intensities in the absence and in the presence of the quenchers (Q = AHs), respectively, τ_0 is the fluorescence lifetime of the fluorophore in the absence of the quenchers, and k_q is the bimolecular

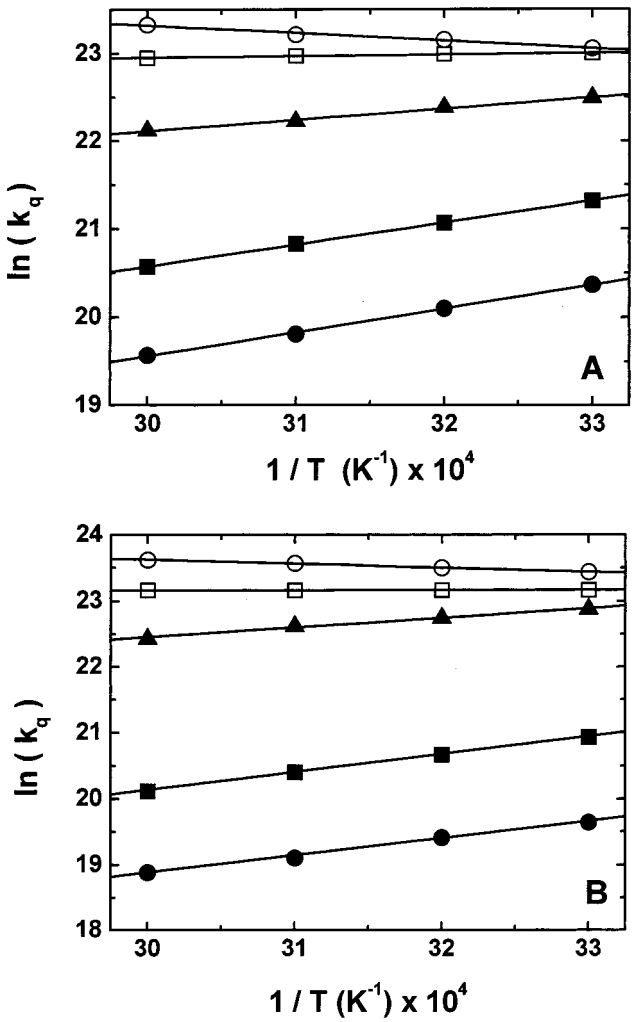

Figure 5. Arrhenius plots (cf. eq 7) for different DHNQ−quencher pairs in (**A**) cyclohexane and (**B**) acetonitrile. The quenchers are XYL (●), MES (■), TMB (▲), PMB (□), and HMB (○).

quenching rate constant. The τ_0 values of DHNQ in both CH and ACN solvents at different temperatures are given in the Footnote of Table 3.

Temperature effect on the DHNQ fluorescence quenching by AHs was also investigated using SS fluorescence measurements. It is observed that only with HMB as the quencher, the quenching rate increases with temperature. The temperature effect on the fluorescence quenching rates with all other quenchers, however, appear unusual. Thus for the latter quenchers, the quenching rate decreases as the temperature is increased. Figures 4A and 4B show the effect of temperature on the SV plots for DHNQ−XYL and DHNQ−HMB pairs in CH, indicating the opposite temperature effects on the quenching rates for the two DHNQ−AH pairs. The temperature-dependent k_q values obtained for different DHNQ−AH systems in CH and ACN are listed in Table 3.

The temperature coefficients of the quenching rates (i.e., ΔE_q) for DHNQ−AH systems were estimated by analyzing the temperature-dependent k_q values using Arrhenius relation (eq 7):[48]

$$\ln k_q = \ln A - \frac{\Delta E_q}{RT} \tag{7}$$

where *A*, *R*, and *T* have their usual meanings. Figures 5A and 5B show the Arrhenius plots for different DHNQ−AH systems in CH and ACN, respectively. The ΔE_q values obtained from the slopes of these plots are listed in Table 2. While the ΔE_q value is positive for HMB, for all other AHs, the ΔE_q values are seen to be negative. With BZ as the quencher, the ΔE_q could not be estimated accurately because of weak fluorescence quenching, though qualitatively the negative temperature effect on the quenching rates is also indicated for the DHNQ−BZ system (cf. footnote of Table 3). It is seen from Table 2 that the negative value of ΔE_q gradually reduces as one moves from the lower to the higher analogues of AHs and the value ultimately becomes positive for HMB. These results thus indicate that the basic nature of the interaction might be the same for all AHs used and the cause for the negative temperature effect on the quenching rates gradually reduces as the quenching strength of AHs is gradually increased making the temperature effect ultimately positive for the strongest AH quencher, HMB (cf. IP and $E(AH/AH^{\cdot+})$ values of AHs; Table 1). We will discuss further the unusual temperature effect on the quenching kinetics latter in section 3.3 in relation to the analysis of the exciplex kinetics.

3.2. Time-Resolved Fluorescence Quenching. The effect of AHs on the fluorescence lifetime (τ) of DHNQ was also investigated in CH and ACN solutions using TR fluorescence measurements. Since the sensitivity of our TR fluorescence setup with a Philips XP-2020Q photomultiplier tube as the detector is quite low at the spectral range of the DHNQ fluorescence, we mostly measured the fluorescence decays without any monochromator but with suitable lower cutoff filters in the emission side of the detection set up. It is observed that for all the AH concentrations used, the observed fluorescence decays fit reasonably well with the single-exponential analysis. Typical fluorescence decay curves as obtained for the DHNQ−HMB system in ACN with different HMB concentrations are shown in Figure 6 along with their single-exponential analysis. It is seen that the observed τ value for the present systems gradually reduces as the AH concentration is increased in the solution. These results thus indicate the dynamic nature of the quenching process in the present systems. Interestingly however, it is seen that the reductions in the τ values with the AH concentrations do not follow the linear SV relation (eq 8)[47] for any of the quenchers used.

$$\frac{\tau_0}{\tau} = 1 + K_{SV}[Q] = 1 + k_q\tau_0[Q] \tag{8}$$

where τ_0 and τ are the fluorescence lifetimes of DHNQ in the absence (cf. footnote of Table 3) and in the presence of the quenchers and [Q] is the quencher concentration used.

For all the DHNQ−AH systems, it is seen from the TR fluorescence quenching results that the τ_0/τ vs [Q] plots always undergo a negative deviation from SV linearity (eq 6) and tend toward a saturation value at very high concentration of the AHs. Though for HMB, we could not attain the saturation condition in τ_0/τ vs [Q] plot due to the limited solubility of the quencher in both CH and ACN (~0.08 mol dm^{-3}), the negative deviation from SV linearity is clearly indicated from the TR quenching results.

The negative deviations in the τ_0/τ vs [Q] plots form the SV linearity clearly indicate that the quenching mechanism for the S_1 state of DHNQ (DHNQ*) by the AHs is a reversible process. Thus, all the DHNQ* molecules interacting at any moment with the AHs do not get quenched, rather a part of these molecules revert back to free DHNQ* by a backward reaction. As a result of this, the fluorescence lifetime of DHNQ* molecules are not reduced to the extent expected if the backward reaction was

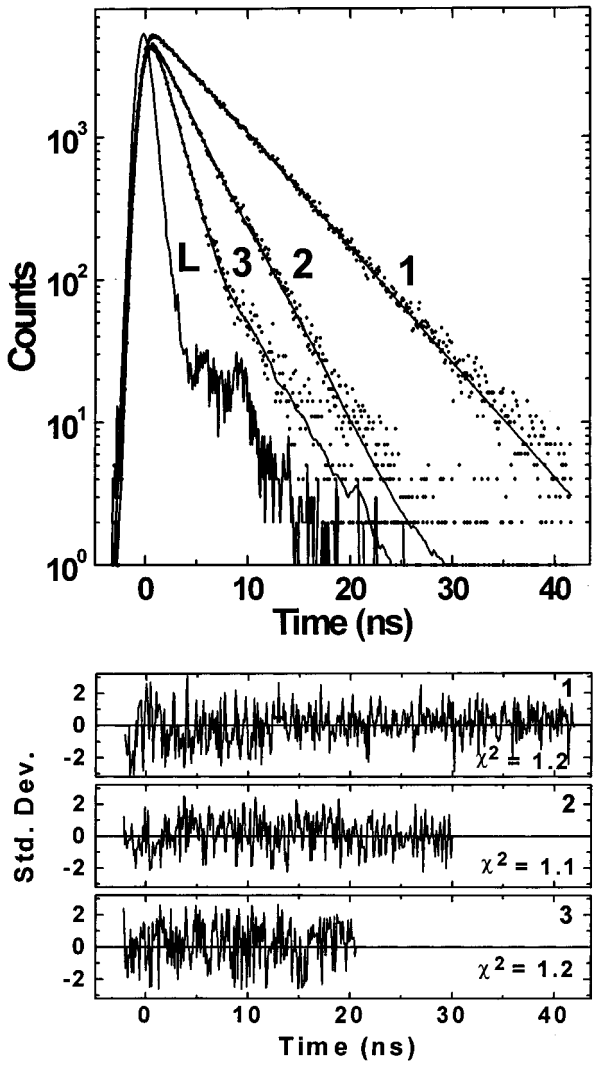

Figure 6. Fluorescence decay curves of DHNQ in acetonitrile solution in the presence of (1) 0, (2) 0.025, and (3) 0.074 mol dm^{-3} of HMB: The dots represent the experimental curves and the continuous lines represent the fitted curves following single-exponential analysis. The curve L represents the instrument response function. The τ values estimated are 5.36, 2.77, and 1.40 ns, respectively, for decay curves 1, 2, and 3. The distributions of the residuals and the χ^2 values corresponding to the single-exponential analysis of the fluorescence decays are shown in the lower panels.

absent in the quenching mechanism. Thus, τ_0/τ vs [Q] plots for the present systems do not follow the linear SV relation (eq 8), rather undergo a negative deviation from the linearity as the quencher concentrations are increased. We suppose that the backward reaction during the interaction of the DHNQ* molecules with the AHs arises due to the involvement of the exciplexes as the intermediates, which can as well dissociate back to produce the reactants, DHNQ* and AH, along with the other deactivation channels of the exciplexes.

Temperature effect on the dynamic quenching behavior was also investigated for all DHNQ−AH systems. For all AHs except HMB, the quenching rate is seen to decrease with temperature. For HMB, however, the dynamic quenching process becomes more efficient as the temperature of the solution is increased. Thus, the temperature effect on the dynamic quenching also goes along with the observations made in the SS quenching measurements. Further, it is seen that at all the temperatures, the τ_0/τ vs [Q] plots do have negative deviations from SV linearity for all AHs used. Typical τ_0/τ vs [Q] plots for DHNQ−MES and DHNQ−HMB pairs in ACN are shown in Figures 7A and 7B, respectively, indicating the opposite temperature effect on the TR fluorescence quenching.

3.3. Analysis of the Exciplex Kinetics for DHNQ−AH Systems. Fluorescence quenching via exciplex formation in the present systems can suitably be presented by the following kinetic scheme (Scheme 1),[27,49] where A*, Q, and (AQ)* represent the excited fluorophore (DHNQ*), the ground-state quencher (AH), and the exciplex, respectively. In Scheme 1, k_1 and k_2 are the radiative and nonradiative decay rate constants of the fluorophore, k_3 and k_4 are the formation and dissociation constants of the exciplex, k_5 and k_6 are the radiative and nonradiative decay rate constants of the exciplex, and k_7 is the sum of the rate constants of all other deactivation channels for the exciplex, namely, ion dissociation (ID), product formation, etc.,

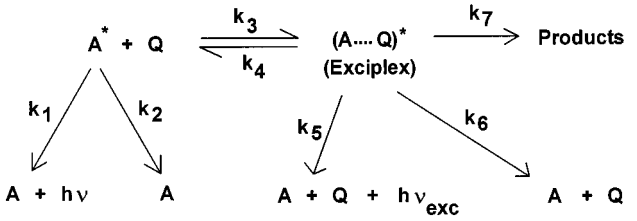

Applying steady-state considerations in Scheme 1, one can easily derive eq 9 for the SS fluorescence intensity quenching of DHNQ by AHs.

$$\frac{I_0}{I} = 1 + \frac{k_3 k_p \tau_0 [Q]}{k_4 + k_p} \tag{9}$$

where,

$$k_p = (k_5 + k_6 + k_7) = \frac{1}{\tau_{exc}} \tag{10}$$

and τ_{exc} is the lifetime of the exciplex, (AQ)*. It is evident from eq 9 that SS fluorescence quenching via the exciplex formation mechanism should follow a linear SV relationship, as experimentally observed for DHNQ−AH systems. Comparing eq 9 with eq 6, the bimolecular quenching constant k_q for the present systems should be expressed as

$$k_q = \frac{k_3 k_p}{k_4 + k_p} \tag{11}$$

According to eq 11, it is evident that for the present systems the observed k_q is not the rate constant of a simple bimolecular quenching step, rather, it is a function of a number of rate constants namely, k_3, k_4, and k_p. The fact that the observed k_q for BZ, TOL, XYL, MES, TMB, and PMB decreases with temperature indicates that the function $(k_4 + k_p)$ increases faster with temperature than the function $(k_3 k_p)$, resulting in an overall negative temperature effect on k_q values for the above quenchers. For HMB the reverse is the situation causing the k_q to increase with temperature.

Considering the TR quenching, following Scheme 1 and assuming a δ-pulse excitation, the time-dependent variations of A* and (AQ)* can be expressed as[27,49]

$$[A^*] = C_1 \exp(-t/\tau_1) + C_2 \exp(-t/\tau_2) \tag{12}$$

$$[(AQ)^*] = C_3 \{\exp(-t/\tau_1) - \exp(-t/\tau_2)\} \tag{13}$$

where τ_1, τ_2, C_1, C_2, and C_3 are the complicated functions of all the rate constants from k_1 to k_7, as well as the concentration of the quencher.[27,49] Thus a biexponential decay for A* and a growth and decay for (AQ)* are expected from eqs 12 and 13. However, under some circumstances, especially when the equilibrium between A* and (AQ)* is established very fast, the biexponential decay for both A* and (AQ)* may not be observed, rather the effective decay of both the species would be close to a single-exponential function with almost similar lifetimes (τ).[49−51] Thus, when k_3[Q] and k_4 are much higher than ($k_1 + k_2$) and k_p values, the equilibrium between A* and (AQ)* should be established very quickly, and the effective fluorescence decay rate constant (k_{eff}) of both the species should be determined by the concentration-weighted average of the independent decay rate constants of A* and (AQ)*. Under such equilibrium conditions, k_{eff} should be expressed as[49,50]

$$k_{eff} = \tau^{-1} = (k_1 + k_2)\left(\frac{[A^*]}{[A^*] + [(AQ)^*]}\right) + k_p\left(\frac{[(AQ)^*]}{[A^*] + [(AQ)^*]}\right)$$

$$= (k_1 + k_2)\left(\frac{k_4}{k_4 + k_3[Q]}\right) + k_p\left(\frac{k_3[Q]}{k_4 + k_3[Q]}\right) \quad (14)$$

Rearranging eq 14, the expression for the observed fluorescence lifetime (τ) in the presence of the quencher is obtained as

$$\tau = \frac{1 + K[Q]}{\tau_0^{-1} + Kk_p[Q]} \quad (15)$$

where K ($= k_3/k_4$) is the equilibrium constant for the exciplex formation. Rearranging eq 15 further in accordance with the SV expression for TR quenching (cf. eq 8), one obtains

$$\frac{\tau_0}{\tau} = \frac{1 + Kk_p\tau_0[Q]}{1 + K[Q]} \quad (16)$$

According to eq 16, the τ_0/τ vs [Q] plots should show negative deviations from SV linearity and tend toward a saturation value of about ($k_p\tau_0$) at very high concentration of the quenchers. This is exactly what we observed in the TR quenching of DHNQ fluorescence by the AHs (cf. Figure 7).

To analyze the TR data for DHNQ fluorescence quenching by AHs, eq 16 may further be rearranged in its linear form as

$$(\tau^{-1} - \tau_0^{-1})^{-1} = K^{-1}(k_p - \tau_0^{-1})^{-1}[Q]^{-1} + (k_p - \tau_0^{-1})^{-1} \quad (17)$$

According to eq 17, a plot of $(\tau^{-1} - \tau_0^{-1})^{-1}$ vs $[Q]^{-1}$ should yield a straight line. Figures 8A and 8B show some typical $(\tau^{-1} - \tau_0^{-1})^{-1}$ vs $[Q]^{-1}$ plots for DHNQ−MES pair in CH and ACN, respectively, at different temperatures. From the slopes and intercepts of such plots, K ($= k_3/k_4$, the equilibrium constant for the exciplex formation) and k_p ($= 1/\tau_{exc}$, the inverse of the exciplex lifetime) values were estimated for different DHNQ−AH pairs in both CH and ACN solutions and are listed in Table 4. It is seen from this table that K value sharply increases as one goes from lower to higher analogues of AHs. It is seen from Table 1 that the electron donating power of the AHs increases as the number of the methyl substituents increases in the benzene ring. Since the exciplexes in the present systems are formed by CT type of interactions, an increase in the K value on going to the higher analogues of the AHs is highly expected. From Table 4 it is seen that unlike K, the k_p values

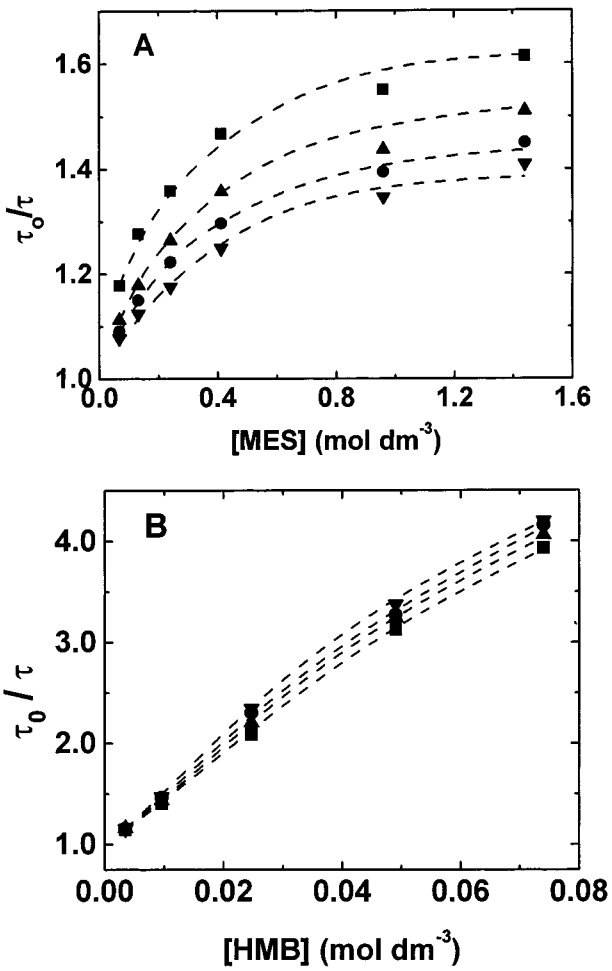

Figure 7. Typical Stern−Volmer plots (τ_0/τ vs [Q], cf. eq 8) obtained from time-resolved quenching studies in (**A**) DHNQ−MES and (**B**) DHNQ−HMB systems in acetonitrile at different temperatures; 30 °C (■), 40 °C (▲), 50 °C (●), and 60 °C (▼).

are only marginally increased as one goes from the lower to the higher analogues of AHs. Since $k_p = (1/\tau_{exc})$, it is indicated from Table 4 that the τ_{exc} values for the present systems fall in the range of about 1 to 5 ns for the temperature range studied.

Another interesting point to be noted from Table 4 is that in both CH and ACN, the k_p (and also K) values are almost in the similar range for any particular DHNQ−AH pair. It is usually expected that in a strongly polar solvent like ACN, the ion-dissociation (ID) process becomes a preferred deactivation channel for the exciplexes, resulting in a higher k_p value in comparison to that in a nonpolar solvent such as CH.[45,46] Similar k_p values for the present systems in both CH and ACN thus indicate that ID is not that favorable for the exciplexes in the present systems. Since the extent of CT in the present exciplexes are quite less (μ_{exc} ~4 to 7 D), it is likely that there is not much of ID for the exciplexes in the present systems even in a strongly polar solvent like ACN.

3.4. Picosecond Laser Flash Photolysis (LFP) Studies. To substantiate the inferences drawn from the fluorescence quenching studies, we carried out the picosecond LFP experiments on different DHNQ−AH systems using 532 nm laser excitation. Since the solubility of DHNQ is quite low in both CH and ACN, and the 532 nm appears only at the longer wavelength tail of the DHNQ absorption spectrum (cf. Inset B of Figure 1), it was not possible to carry out the LFP experiments for the present systems in either of the above solvents using 532 nm laser excitation. We thus used benzonitrile (BZN) as the solvent to

TABLE 4: Rate Parameters Determined from the Temperature Dependent Steady-State and Time-Resolved Quenching for Different DHNQ-AH Systems in Cyclohexane (CH) and Acetonitrile (ACN) Solutions

		CH		ACN	
AH	temp. (°C)	K ($dm^3\,mol^{-1}$)	k_p ($10^9\,s^1$)	K ($dm^3\,mol^{-1}$)	k_p ($10^9\,s^{-1}$)[a]
TOL	30	0.74	0.28	0.41	0.25
	40	0.66	0.27	0.38	0.24
	50	0.61	0.26	0.36	0.23
	60	0.57	0.26	0.30	0.22
XYL	30	1.25	0.38	0.86	0.28
	40	1.05	0.35	0.85	0.27
	50	0.93	0.32	0.84	0.26
	60	0.87	0.30	0.83	0.25
MES	30	4.19	0.37	3.70	0.32
	40	3.45	0.35	3.41	0.29
	50	2.76	0.34	3.00	0.28
	60	2.04	0.33	3.10	0.27
TMB	30	9.7	0.84	17.5	0.66
	40	9.4	0.75	17.1	0.61
	50	9.3	0.68	16.2	0.56
	60	9.0	0.63	14.3	0.54
PMB	30	10.1	1.00	14.0	0.97
	40	9.5	0.96	13.3	0.94
	50	9.3	0.90	13.0	0.91
	60	9.2	0.81	12.6	0.87

[a] Following Scheme 1, $\tau_{exc} = k_p^{-1}$(cf. eq 10).

carry out the LFP experiments for the present systems, as the solubility of DHNQ in BZN is reasonably high.

Time-resolved transient absorption spectra as obtained for DHNQ in BZN in the presence of 0.5 mol dm^{-3} PMB are shown in Figure 9. Immediately after photoexcitation, one broad absorption band appears in the 530 to 630 nm region, with a peak at around 600 nm and a shoulder at around 560 nm. There is also a weak longer wavelength absorption tail in the transient absorption spectra extending beyond about 800 nm. The transient absorbance is seen to decrease with time, without showing any change in the shape of the spectra. For the 530−630 nm region, the transient decay time constant k_{ps} was estimated following first-order kinetic analysis of the time-dependent transient absorptions. The value of k_{ps} thus estimated ($\sim 6 \times 10^8\ s^{-1}$) seems to be about an order of magnitude lower than the pseudo first-order rate constant ($k = k_q[Q] \approx 5 \times 10^9\ s^{-1}$) expected following SS fluorescence quenching results with PMB. For the longer wavelength absorption tail (~650−800 nm), the transient decay time could not be estimated due to very weak absorptions. The picosecond LFP results with other quenchers were very similar to those obtained with PMB.

The picosecond LFP experiments were also carried out for DHNQ using BZ, TOL, XYL and MES directly as the solvents. In all these cases the LFP results were qualitatively very similar to those obtained in BZN solution. These results thus indicate that similar transients are produced following 532 nm LFP of DHNQ−AH systems in BZN solution or DHNQ in neat aromatic solvents.

From the solvent polarity effect on the exciplex emission maxima (cf. section 3.1) we inferred that the S_1 state of DHNQ undergoes a CT type of interaction with the AHs. It is possible that the transients produced in the picosecond LFP studies may be either the S_1 state of DHNQ, the anion radical of DHNQ (i.e., $DHNQ^{\cdot-}$) or the cation radical of the AH ($AH^{\cdot+}$). The $AH^{\cdot+}$ radical cations mostly absorb in the spectral range < 500 nm.[52] Thus none of the transient absorption bands in the 530 to 800 nm region could not assigned to the $AH^{\cdot+}$ radicals. This is

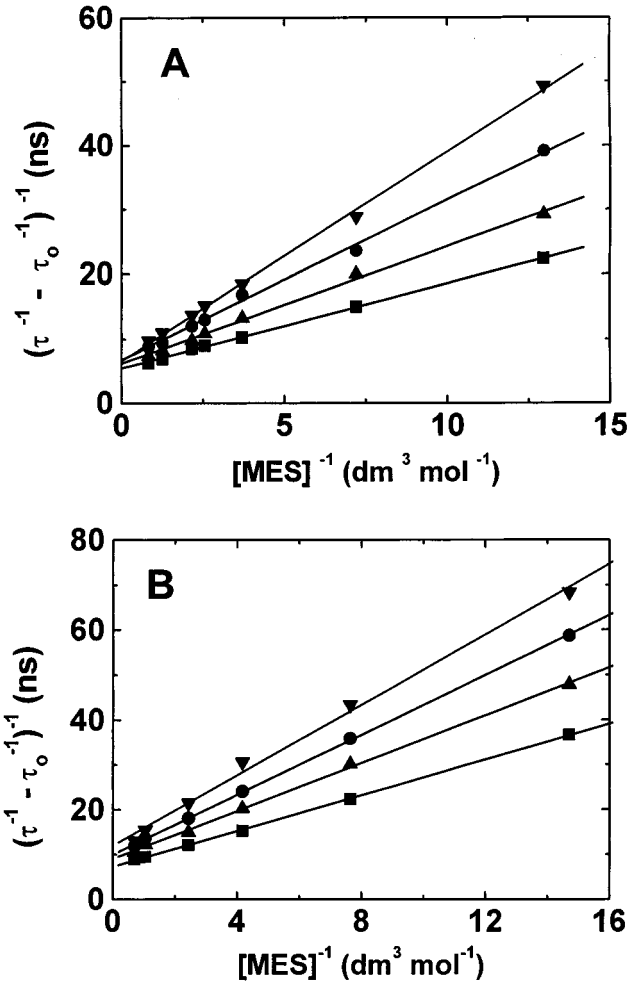

Figure 8. The $(\tau^{-1} - \tau_0^{-1})^{-1}$ vs $[MES]^{-1}$ plots (cf. eq 17) in (**A**) cyclohexane and (**B**) acetonitrile at different temperatures: 30 °C (■), 40 °C (▲), 50 °C (●), and 60 °C (▼).

further substantiated by the fact that irrespective of the AH used, the shape and the peak positions of the transient absorption spectra remained invariant. To the best of our knowledge, the absorption spectrum of $DHNQ^{\cdot-}$ radical is not reported in the literature. Assuming that the absorption spectrum of $DHNQ^{\cdot-}$ will not differ much from that of the anion radical of its lower analogue, QZ (i.e., $QZ^{\cdot-}$), the absorption band in the 530 to 630 nm region cannot be attributed to the $DHNQ^{\cdot-}$ radical anion. It is to be noted that the $QZ^{\cdot-}$ radical anion has a strong absorption peak at around 475 nm and a weak absorption tail in the 600 to 800 nm region.[53] From the present LFP results it is indicated that the transient absorptions in the 530−630 nm region must be due to the S_1 to S_n absorptions of DHNQ. The fact that the transient decay times in the 530−630 nm absorption band are about an order of magnitude lower than the expected $k_q[Q]$ values for all DHNQ−AH systems clearly indicates the involvement of the exciplexes as the intermediates in the present systems. Because the exciplexes can produce back the S_1 state of DHNQ by a reverse reaction (step k_3; Scheme 1), the apparent lifetime of the S_1 state of DHNQ becomes relatively longer than what it would have been if the reverse reaction was absent in the quenching mechanism.

The transient responsible for the long absorption tail in the 650−800 nm region in the picosecond transient absorption spectra is not very clear to us. We suppose that this absorption

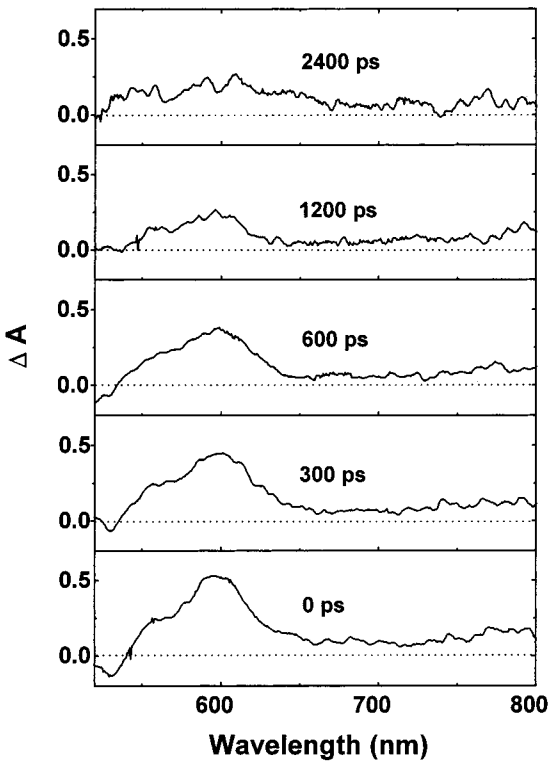

Figure 9. Picosecond transient absorption spectra of DHNQ−PMB pair in benzonitrile. The PMB concentration used was 0.5 mol dm^{-3}. The time delays between the pump and probe pulses for different transient absorption spectra are indicated in the figure.

tail could be due to the $DHNQ^{\cdot-}$ anion radicals, produced due to direct ET from AHs to a fraction of the excited DHNQ molecules.[53]

It is interesting at this point to compare the k_{ps} values obtained from the analysis of the 530−630 nm transient absorption decays in the picosecond LFP experiments with the k_p ($= 1/\tau_{exc}$) values obtained from the exciplex analysis of the SS and TR fluorescence quenching results. Such a comparison reveals that for all DHNQ−AH systems, k_{ps} values are in the similar range as the k_p values. From eqs 15 and 16, it is evident that the S_1 state lifetime of DHNQ in the presence of very high concentration of AH should attend a limiting value of about k_p, the inverse of the exciplex lifetime, τ_{exc}. Since in the picosecond LFP experiments we used reasonably high concentration of the AHs ($\sim$0.5 mol dm^{-3} or more), the similarities in k_{ps} and k_p values clearly indicate that the transient absorbing in the 530−630 nm region must be the S_1 state of DHNQ. That the S_1 state of DHNQ does not decay as fast as expected from k_q values obtained from the SS fluorescence quenching results (cf. Table 3) indicate that the mechanism of interaction of the S_1 state of DHNQ with the AHs is a reversible process. The reversibility in the quenching mechanism arises due to the involvement of the exciplexes as the intermediates for the present systems. Thus, the picosecond transient absorption results are seen to be exactly in accordance with the inferences drawn from the SS and TR fluorescence quenching studies.

3.5. Exciplex Formation versus Direct Electron Transfer in DHNQ−AH Systems. In most of the donor−acceptor systems, it is usually seen that the exciplexes are mainly formed in nonpolar solvents.[42−46,51] In strongly polar solvents, however, the exciplexes are often very unstable due to their fast dissociation to the solvent-separated ions.[45,46] Further, in a strongly polar solvent like ACN, direct ET from the donor to the acceptor often dominates over the exciplex formation.[43−45] The exciplex emissions are thus hardly observed in ACN solutions for most donor−acceptor systems. For the present DHNQ−AH systems, it is seen that the exciplex emissions in ACN are almost comparable to those in the nonpolar CH solvent. These observations thus indicate that for the present systems the direct ET may not be contributing much to the observed quenching rates even in ACN solution.

One interesting point, however, to be noted from Table 3 is that the k_q values with stronger quenchers such as TMB, PMB, and HMB are higher in polar solvent ACN than in nonpolar solvent CH. The reverse is the case with weaker quenchers such as BZ, TOL, XYL, and MES. The higher k_q values in CH than in ACN for BZ, TOL, XYL, and MES indicate that the quenching of DHNQ fluorescence by these quenchers could be solely due to the exciplex mechanism. Since the exciplex formation is usually favored in a nonpolar solvent,[42−46,51] the quenching process becomes more efficient in CH than in ACN, as observed for the weak quenchers such as BZ, TOL, XYL, and MES. For stronger quenchers such as TMB, PMB, and HMB, however, the higher k_q values in ACN than in CH indicate that in the former solvent direct ET mechanism might also be contributing to some extent along with the exciplex mechanism. It is to be noted, however, that the major contribution toward the fluorescence quenching of DHNQ by TMB, PMB, and HMB comes through the exciplex mechanism even in the strongly polar solvent ACN. For weaker quenchers such as BZ, TOL, XYL, and MES, the fluorescence quenching results indicate that the quenching could be solely due to the exciplex mechanism in both nonpolar and polar solvents.

The differences in the quenching results for stronger and weaker quenchers in polar and nonpolar solvents can be understood qualitatively by considering the solvation of the reactants, intermediates, and the product states. In a strongly polar solvent like ACN, it is likely that both donor (D) and acceptor (A*) will diffuse to each other along with their solvation shell, which is supposed to be strongly held around the reactants. It is thus expected that the encounter complex initially formed between D and A* will always have an intervening solvent layer between them. ET can directly take place in this encounter complex to give the solvent separated ion pair (SSIP) if the free energy change ($\Delta G°$) permits ET reaction to occur with a reasonable rate. The other route of reaction in the encounter complex is to form the exciplex through the rearrangement of the intervening solvent layer so that the donor and the acceptor can come in physical contact for the exciplex formation.[45,46] We feel that with strong quenchers such as TMB, PMB, and HMB, the rate of direct ET is reasonable enough in comparison to the reaction rate through exciplex channel and thus shows its contribution in the observed quenching rate. For weak quenchers such as BZ, TOL, XYL, and MES, the rate of direct ET could be very low and thus DHNQ fluorescence quenching mainly occurs via the exciplex channel.

In a nonpolar solvent such as CH, the solvent layers around the reactants are expected to be weakly held. It is thus likely that during the formation of the encounter complex, the solvent layer between the donor and the acceptor can largely be excluded, making the reactants come in physical contact. In a nonpolar solvent, the encounter complex can quickly switch over to the exciplex state before ET can take place. It is thus expected that in a nonpolar solvent the interaction should be mostly due to the exciplex formation.

Due to the solvent intervention, the rate of exciplex formation is expected to become slower in polar solvents. Thus the

observed k_q in ACN (SS results, cf. Table 3) is lower than in CH with weak quenchers such as BZ, TOL, XYL, and MES, for which the probability of ET is expected to be very low from the energetic ($\Delta G°$) consideration. For stronger quenchers such as TMB, PMB, and HMB, it is reasonable to assume that the rate of ET is not that negligible and can contribute to some extent along with the exciplex channel to quench the DHNQ fluorescence. This explains why k_q values in ACN are higher than in CH for stronger quenchers such as TMB, PMB, and HMB (cf. Table 3). That direct ET also contributes to some extent in DHNQ−AH systems is indicated from the appearance of the longer wavelength absorption tail (in 650−800 nm region) in the picosecond LFP studies, which we attributed to $DHNQ^{\cdot-}$ anion radical (cf. section 3.4) comparing the anion radical absorption spectrum of QZ.[53] From the present results we infer that for DHNQ−AH systems, though the exciplex mechanism is the major channel for DHNQ fluorescence quenching, direct ET process can also contribute to some extent depending on the donor strength of AHs and the polarity of the solvent used.

3.6. Exciplex Formation and the Associated Free Energy Changes. At this point it is interesting to discuss on the energetics of the exciplex formation in the present systems. From the redox potentials of DHNQ and AHs, it is seen that $\{E(\mathrm{AH/AH^{\bullet+}}) - E(\mathrm{Q/Q^{\bullet-}})\} > E_{00}{}^{\mathrm{Q}}$ of DHNQ*. Thus, apparently it seems that the CT interaction between DHNQ* and AHs is not favorable. If one considers a complete ET from AHs to DHNQ*, the free energy changes should be given as,[54,55]

$$\Delta G_{\mathrm{et}} = \{E(\mathrm{AH/AH^{\bullet+}}) - E(\mathrm{Q/Q^{\bullet-}})\} - E_{00}{}^{\mathrm{Q}} + C \qquad (18)$$

where C is Coulomb interaction energy in the ion-pair formed by ET. Since under diffusive conditions the bimolecular ET processes results in the formation of solvent separated ion-pairs (SSIP),[54,55] the interaction energy C should be given by

$$C = -\frac{e^2}{\epsilon\, r_{\mathrm{DA}}} \qquad (19)$$

where r_{DA} is the separation (∼7 Å) between $AH^{\cdot+}$ and $Q^{\cdot-}$ in the SSIP. Thus, C is quite small (∼0.05 eV) for the ET reaction in polar solvent such as ACN.[54,55] For the present systems, it is thus indicated from eqs 18 and 19 that the ET processes are highly endergonic. However, even in the endergonic cases such as the present ones, the ET processes are often seen to occur with reasonable rates as the SSIP states formed by ET usually undergo faster decay via nonradiative return ET compared to the independent decay of the excited fluorophore.[42−45,54,55] Thus, fluorescence quenching by ET mechanism even for the endergonic cases are not uncommon.[42−45] In the present DHNQ−AH systems, it is indicated from the fluorescence quenching results that along with the exciplex mechanism some direct ET also contribute in polar ACN solvent, especially with relatively stronger AH donors (cf. section 3.5).

In the case of exciplex formation, the redox characteristics of D and A are not the only criteria, as the exciplexes are usually formed at the close contact of the reactants.[54,55] If both D and A are of planar organic molecules, as are the present cases, the exciplexes are preferentially formed by a face-to-face geometry of the reactants, with interaction distance r_{cc} (∼3−4 Å) much smaller than r_{DA} in SSIP state.[54,55] Further, with face-to-face geometry, there is a favorable orbital interaction between D and A* along with the Coulombic interaction due to charge transfer (CT) from D to A* to stabilize the exciplexes.[54,55] Since for the present systems $E_{00}{}^{\mathrm{D}} > E_{00}{}^{\mathrm{A}}$ and the dipole moments (μ_{exc}) of the exciplexes are not very high, the wave function of the exciplexes can suitably be presented as[54,55]

$$\psi_{\mathrm{EX}} \approx C_1\psi(\mathrm{DA^*}) + C_3\psi(\mathrm{D^+\,A^-}) \qquad (20)$$

It is indicated from eq 20 that both locally excited state ψ(DA*) and the CT state $\psi(D^+A^-)$ contribute appreciably to the overall wave function of the exciplex. Such exciplexes are usually emissive in nature, though the nonradiative deactivation channel often dominates in the exciplexes.[54,55] If both D and A have very strong electron donating and accepting powers, respectively, (it is not the case for the present systems), it is expected that the $\psi(D^+A^-)$ state will mainly contribute in ψ_{EX}, resulting in the formation of an exciplex with just the contact ion-pair (CIP) character. Such species are usually nonemissive in nature.[54,55] It is indicated from eqs 20 that as long as D and A have different electron donating and accepting powers, the CT state $\psi(D^+A^-)$ will always contribute to some extent, causing the exciplexes to be formed with some CT character. If both D and A are having exactly the similar electron donating and accepting powers, as in the cases of excimers, the exciplexes will not display any CT character.[54,55]

The free energy changes for exciplex formation in the present systems can conveniently be presented as[54,55]

$$\Delta G_{\mathrm{EX}} = \{E(\mathrm{AH/AH^{\bullet+}}) - E(\mathrm{Q/Q^{\bullet-}})\} - E_{00}{}^{\mathrm{Q}} + C + \frac{e^2}{2}\left(\frac{1}{r_{\mathrm{D}}} + \frac{1}{r_{\mathrm{A}}}\right)\left(1 - \frac{1}{\epsilon}\right) + E_{\mathrm{orb}} - \frac{\mu_{\mathrm{exc}}{}^2}{\rho^3}\left(\frac{\epsilon - 1}{2\epsilon + 1}\right) \qquad (21)$$

where E_{orb} is the interaction energy (−ve) due to orbital overlap of D and A*. For exciplexes, the Coulomb energy C should approximately be given as

$$C \approx -\frac{e^2}{r_{\mathrm{cc}}} \qquad (22)$$

because, at the face-to-face close contact there is no solvent shielding between D^+ and A^- in the CIP.[54,55] Thus the term C contributes appreciably in the stabilization of the exciplexes. Another stabilization factor for the exciplexes comes through the interaction of the polar solvent with the dipole of the exciplexes (μ_{exc}). Though the exact ΔG_{EX} is not possible to calculate, it is indicated from eq 21 that the stable exciplexes with CT character can be formed for the present systems even if the $E_{00}{}^{\mathrm{Q}}$ energy is less than $\{E(\mathrm{AH/AH^{\bullet+}}) - E(\mathrm{Q/Q^{\bullet-}})\}$ for the donor−acceptor systems.

4. Conclusions

The fluorescence of DHNQ is quenched by AHs via the formation of exciplexes in both nonpolar (CH) and polar (ACN) solvents. The results indicate that the exciplexes are formed between the excited (S_1) state of DHNQ and the ground state of AHs by the CT type of interaction. The estimated dipole moments of the exciplexes (μ_{exc} about 4 to 7 D), however, indicate that the extent of CT is not that large in the present systems. The kinetic information in relation to the exciplex formation in the present systems has been obtained from the analysis of the SS and TR fluorescence quenching results following a suitable mechanistic scheme. In a strongly polar solvent such as ACN, the quenching rate constants are higher than in nonpolar CH solvent for stronger quenchers such as TMB, PMB, and HMB, though the results are just opposite for rest of the weaker AH quenchers, such as BZ, TOL, XYL, and MES. We infer from these results that for strong AH quenchers in polar solvent, a direct ET process also contributes to some

extent along with the exciplex channel to quench the DHNQ fluorescence. Relative importance of the ET and the exciplex formation channels in polar and nonpolar solvents has been explained considering the possible solvent intervention during the encounter of the donor and the acceptor prior to the exciplex formation for the ET reaction. The present DHNQ−AH systems are found to be among those rare donor−acceptor pairs for which reasonable exciplex emissions are seen even in a strongly polar solvent such as ACN.

References and Notes

(1) Rembold, M. W.; Kramer, H. E. A. *J. Soc. Dyers Colour*. **1980**, *96*, 122.

(2) Bordie, A. F. In *Biochemistry of Quinones*; Morton, R. A., Ed.; Academic Press: New York, 1965.

(3) Brown, J. R. In *Progress in Medicinal Chemistry*; Ellis, G. P., West, G. B., Eds.; North-Holland: Amsterdam, 1978; Vol. 15.

(4) Kalyanraman, B.; Perez-Reyes, E.; Mason, R. P. *Biochim. Biophys. Acta* **1980**, *630*, 119.

(5) Remers, W. A. *The Chemistry of Antitumour Antibiotics*; Wiley-Interscience: New York, 1979; Vol. 1, Chapter 2.

(6) Butler, J.; Hoey, B. M. *Br. J. Cancer* (suppl-III) **1987**, *55*, 53.

(7) Mukherjee, T. *Proc. Indian Acad. Sci*. **2000**, *66A*, 239.

(8) Giles, C. H.; Sinclair, R. S. *J. Soc. Dyers Colour*. **1972**, *88*, 109, and **1973,** *89*, 56.

(9) Egerton, G. S.; Assaad, O. N. E. N. *Chem. Ind. (London)* **1967**, *50*, 2112.

(10) Palit, D. K.; Pal, H.; Mukherjee, T.; Mittal, J. P. *J. Chem. Soc., Faraday Trans*. **1990**, *86*, 3861.

(11) Rasimas, J. P.; Blanchard, G. J. *J. Phys. Chem*. **1995**, *99*, 11338.

(12) Hibbert, F.; Spiers, K. J. *J. Chem. Soc., Perkin Trans. II* **1987**, 1617.

(13) Inoue, H.; Hida, M.; Nakashima, N.; Yoshihara, K. *J. Phys. Chem.* **1982**, *86*, 3184.

(14) Flom, S. R.; Barbara, P. F. *J. Phys. Chem.* **1985**, *89*, 4489.

(15) Pal, H.; Mukherjee, T.; Mittal, J. P. *Radiat. Phys. Chem*. **1994**, *44*, 603.

(16) Pal, H.; Palit, D. K.; Mukherjee, T.; Mittal, J. P. *Radiat. Phys. Chem.* **1992**, *40*, 529.

(17) Pal, H.; Palit, D. K.; Mukherjee, T.; Mittal, J. P. *J. Chem. Soc., Faraday Trans*. **1991**, *87*, 1109.

(18) Rath, M. C.; Pal, H.; Mukherjee, T. *J. Chem. Soc., Faraday Trans*. **1996**, *92*, 1891.

(19) Land, E. J.; Lexa, D.; Bensasson, R. V.; Gust, D.; Moore, T. A.; Moore, A. L.; Liddell, P. A.; Nemeth, G. A. *J. Phys. Chem*. **1987**, *91*, 4831.

(20) Braun, A. M.; Hubig, S. M.; Rodgers, M. A. J.; Wade, W. H. *Nucl. Instrum. Methods Phys. Res*. **1991**, *61*, 429.

(21) doMonte, S. A.; Braga, M. *Chem. Phys. Lett.* **1998**, *290*, 136.

(22) Hubig, S. M.; Kochi, J. K. *J. Am. Chem. Soc*. **1999**, *121*, 1688.

(23) Pal, H.; Palit, D. K.; Mukherjee, T.; Mittal, J. P. *J. Chem. Soc., Faraday Trans*. **1993**, *89*, 683.

(24) Ghosh, H. N.; Pal, H.; Palit, D. K.; Mukherjee, T.; Mittal, J. P. *J. Photochem. Photobiol. A: Chem*. **1993**, *73*, 17.

(25) Palit, D. K.; Pal, H.; Mukherjee, T.; Mittal, J. P. *Chem. Phys*. **1988**, *126*, 441.

(26) Rath, M. C.; Mukherjee, T. *J. Chem. Soc., Faraday Trans*. **1997**, *93*, 3331.

(27) Birks, J. B. In *Photophysics of Aromatic Molecules*; Wiley-Interscience: New York, 1970.

(28) O'Connor, D. V.; Phillips, D. *Time-Correlated Single Photon Counting*; Academic Press: New York, 1984.

(29) Ghosh, H. N.; Pal, H.; Sapre, A. V.; Mittal, J. P. *J. Am. Chem. Soc*. **1993**, *115*, 11722.

(30) In *CRC Handbook of Chemistry and Physics*, 80th ed.; Lide, D. R., Ed.; CRC Press: Boca Raton, FL, 1999−2000.

(31) In *Encyclopedia of Electrochemistry of the Elements*; Bard, A. J., Ed.; Marcel Dekker: New York, 1978; Vol. 11.

(32) Beens, H.; Knibbe, H.; Weller, A. *J. Phys. Chem*. **1967**, *47*, 1183.

(33) Spears, K. G.; Gray, T. H.; Huang, D. In *Picosecond Phenomena III*; Eisenthal, K. B., Hochstrasser, R. M., Kaiser, W., Laubereau, A., Eds.; Springer-Verlag: Heidelberg, 1982; p 278.

(34) Masuhara, H.; Hino, T.; Mataga, N. *J. Phys. Chem*. **1975**, *79*, 994.

(35) Hirata, Y.; Kanda, Y.; Mataga, N. *J. Phys. Chem*. **1983**, *87*, 1662.

(36) Masuhara, H.; Mataga, N. *Acc. Chem. Res*. **1981**, *14*, 312.

(37) Rath, M. C.; Pal, H.; Mukherjee, T. *J. Phys. Chem*. **1999**, *103*, 4993.

(38) Nath, S.; Pal, H.; Sapre, A. V. *Chem. Phys. Lett.* **2000**, *327*, 143.

(39) Nad, S.; Pal, H. *J. Phys. Chem. A* **2001**, *105*, 1097.

(40) Edward, J. T. *J. Chem. Educ*. **1970**, *47*, 261.

(41) Gastilovich, E. A.; Golitsina, L. V.; Kryuchkova, G. T.; Shigorin, D. N. *Opt. Spektrosk.* **1976**, *40*, 457.

(42) Kuzmin, M. G. *J. Photochem. Photobiol., A. Chem*. **1996**, *102*, 51.

(43) Kikuchi, K.; Niwa, T.; Takahashi, Y.; Ikeda, H.; Miyashi, T.; Hoshi, M. *Chem. Phys. Lett*. **1990**, *173*, 421.

(44) Kikuchi, K.; Takahashi, Y.; Katagiri, T.; Niwa, T.; Hoshi, M.; Miyashi, T. *Chem. Phys. Lett*. **1991**, *180*, 403.

(45) Kavarnos, G. J.; Turro, N. J. *Chem. Rev*. **1986**, *86*, 401.

(46) Baggot, J. E. In *Photoinduced Electron-Transfer Reactions*; Chanon, M., Fox, M. A., Eds.; Elsevier: New York, 1988; Part B, Chapter 2.8, p 385.

(47) Lakowicz, J. R. *Principles of Fluorescence Spectroscopy*; Plenum Press: New York, 1983.

(48) Atkins, P. W. *Physical Chemistry*, 5th ed.; Oxford University Press: Oxford, 1995.

(49) Ware, W. R.; Watt, W.; Holmes, J. D. *J. Am. Chem. Soc*. **1974**, *96*, 7853.

(50) Pal, H.; Palit, D. K.; Mukherjee, T.; Mittal, J. P. *J. Photochem. Photobiol., A Chem*. **1990**, *52*, 391.

(51) Konijnenberg, J.; Huizer, A. H.; Chaudron, F. Th.; Varma, C. A. G. O.; Marciniak, B.; Paszyc, S. *J. Chem. Soc., Faraday Trans. 2* **1987**, *83*, 1475.

(52) Shida, T. *Electronic Absorption Spectra of Radical Ions*; Elsevier: Amsterdam, 1988 (in Physical Science Data).

(53) Mukherjee, T.; Swallow, A. J.; Guyan, P. M.; Bruce, J. M. *J. Chem. Soc., Faraday Trans*. **1990**, *86*, 1483.

(54) Kavarnos, G. J. In *Topics in Current Chemistry*; Mattay, J., Ed.; Springer-Verlag: Berlin, 1990; Vol. 156, p 21.

(55) Kavarnos, G. J. Fundamentals of Photoinduced Electron Transfer; VCH Publishers: New York, 1993.